

Primal and Dual Problems in Electrical Impedance Imaging

Nick Polydorides*

Department of Electrical and Computer
Engineering
University of Cyprus
75 Kallipoleos Ave., Nicosia, Cyprus
nick.polydorides@ucy.ac.cy

Charalambos D. Charalambous**

Department of Electrical and Computer
Engineering
University of Cyprus
75 Kallipoleos Ave., Nicosia, Cyprus
chadcha@ucy.ac.cy

Abstract—Ill-posed inverse boundary value problems are usually approached as problems of inference under a given set of boundary observations. The parameters and data are modelled as random variables so that to encompass the uncertainty of their actual values. This uncertainty is expressed in probability distributions of the variables which are subsequently conjuncted to form the basis of the regularized inverse problem. In this work, we consider the linearized inverse conductivity problem, also known as electrical impedance imaging problem, where a finite set of noise infused boundary voltage measurements is used to reconstruct the conductivity distribution in the interior of simply connected domains. We derive the primal and dual problems in the generalized Tikhonov formulation, and cast the linearized inverse problem as a quadratic optimization problem with an inequality ℓ_2 norm constraint. We show that Tikhonov regularization can be implemented in the context of primal-dual interior point methods to yield optimal images and regularization parameters with respect to the choice of prior information equations and the noise level in the data. The approach can be extended in nonlinear trust-region regularization using algorithms based on consecutive linearization steps.

I. INTRODUCTION

IN Electrical Impedance Imaging (EII), a finite number of electrodes are positioned at the boundaries of closed conducting domains, and while some of them are used to inject low-frequency current patterns into the domain, others record readings of the induced voltage potential. In the image reconstruction problem, the interior conductivity distribution must be recovered using the acquired noise-infused boundary measurements. This nonlinear problem is radically ill-posed and therefore a regularization technique is necessitated in order to yield a stable and unique solution. In order to solve the inverse problem, one should attend first to the forward problem of computing the boundary Dirichlet data when the domain's interior electrical properties and the excitation boundary conditions are known. For a more detailed explanation on the technique and the current status of the development in the image reconstruction in impedance imaging we refer the interested reader to the recent review [14].

*N. Polydorides acknowledges the University of Cyprus for the support of the project Convergence of communication, control and statistical mechanics with applications to network sensors and tele-operation.

**C.D. Charalambous is also with the School of Information Technology and Engineering, University of Ottawa, 161 Louis Paster, A519, Ottawa, Ontario K1N 6N5, Canada.

The technology of EII or electrical impedance tomography (EIT) is now applied in various fields such as biomedical imaging, industrial process monitoring by means of nondestructive testing and geophysics. In biomedicine, EII applications include functional brain imaging, detection of epilepsy, internal hemorrhage and mammography. More information on these tomographic techniques and applications and results can be found in [10], [6] and [4]. In the industrial environment, impedance tomography systems are already in use for monitoring chemical processes, industrial filters, fluidized beds and gas-liquid separators [26].

II. THE FORWARD ELECTROSTATIC PROBLEM

Let $\Omega \subset \mathbf{R}^n$, $n = 2, 3$ a simply connected bounded domain with smooth boundary $\partial\Omega$ and continuous isotropic electrical conductivity \mathbf{x} . In the low-frequency range, Maxwell's time-harmonic equations reduce to the elliptic partial differential equation

$$\nabla \cdot (\mathbf{x}\nabla u) = 0 \quad \text{in } \Omega \quad (1)$$

where u is the scalar voltage potential within the domain. If $\Gamma_1 \subset \partial\Omega$ is the subset of the boundary underneath the L disjoint electrodes, so that $\partial\Omega = \Gamma_1 \cup \Gamma_2$ and Γ_2 is the inter-electrode gap, then the current density on the surface of the l 'th electrode driving a current of magnitude I_l into the domain is given by

$$\int_{L_l} \mathbf{x}\nabla u \cdot \hat{\mathbf{n}} \, ds = \begin{cases} I_l & \text{on } \Gamma_1 \\ 0 & \text{on } \Gamma_2. \end{cases} \quad (2)$$

for $l = 1, \dots, L$. In the above L_l denotes the surface of the l 'th electrode and $\hat{\mathbf{n}}$ the outward unit normal on $\partial\Omega$ as indicated in the schematic diagram 1. The voltage measurement V_l recorded by the l 'th electrode is given by

$$u + z_l \mathbf{x}\nabla u \cdot \hat{\mathbf{n}} = V_l \quad \text{on } \Gamma_1 \quad (3)$$

where z_l denotes the electrode's contact impedance. The model (1)-(3), also known as the complete electrode model [24], admits a unique solution when the Dirichlet (ground) condition $u|_{L_g} = 0$ and the charge conservation principle $\sum_{i=1}^l I_i = 0$ are enforced [21], [13]. For the derivation of the forward problem we introduce the following Sobolev spaces for the data and the parameters. For the conductivity and potential distributions we assume $\mathbf{x} \in L^2(\Omega)$ and $u \in H^1(\Omega)$

respectively, therefore for the boundary currents I_l and measurements V_l the Hilbert spaces $H^{-1/2}(\Gamma_1)$ and $H^{1/2}(\Gamma_1)$ are appropriate. The measurements are to be understood in terms of a trace operator acting on u . In domains with arbitrary boundary shape and complicated interior structure the forward problem is often approached numerically using a finite element method. The description of the numerical approximation methods is outside the scope of this paper so it suffices to mention that the forward problem was solved using the EIDORS package, which implements the complete electrode model using Galerkin method, assuming piecewise constant conductivity and potential in the expansion of linear nodal Lagrangian functions [17]. For more details on the technology of finite elements and the various electrode models in impedance imaging we refer the reader to [24], [11] and [16].

From the solution of the forward problem, we extract the injective, self-adjoint and positive definite Neumann to Dirichlet mapping operator $\Lambda_{\mathbf{x}} := H^{-1/2}(\Gamma_1) \rightarrow H^{1/2}(\Gamma_1)$ which lays the foundations for the inverse problem. It was Calderón who proved the injectivity of $\Lambda_{\mathbf{x}}$ in the linearized impedance imaging problem and showed that the complete knowledge of $\Lambda_{\mathbf{x}}$ in the continuum setting, uniquely determines the distribution of the interior conductivity[5]. In sequence, we proceed to form the nonlinear forward operator $F := L^2(\Omega) \rightarrow H^{1/2}(\Gamma_1)$, so that to relate the parameters of interest to their corresponding boundary observations [17]

$$F(\mathbf{x}) = \mathbf{y}^{exact} + \varepsilon = \mathbf{y} \quad (4)$$

Throughout the paper we assume that \mathbf{y} are measurements contaminated with a noise signal w of level w so that $0 < \|\mathbf{y} - F(\mathbf{x}^*)\|_{H^{-1/2}(\Gamma_1)} \leq w$ and $\mathbf{y} \notin R(F)$.

III. THE INVERSE PROBLEM

In the discrete case, where $\mathbf{x} = \{x^i\}_{i=1}^k$ and $\mathbf{y} = \{y^j\}_{j=1}^m$, we allow \mathcal{X} and \mathcal{Y} to be the parameter and data spaces, and consider that these are finite dimensional linear spaces with *independent homogeneous* and constant probability densities $\mu_{\mathbf{x}}(\mathbf{x})$ and $\mu_{\mathbf{y}}(\mathbf{y})$ respectively. To enhance comprehension of the material to follow we include a small introduction on the main concepts involved in our analysis, in the approach of [22]. Let \mathcal{X} be a finite dimensional manifold to which we assign the notion of volume. Independently of any probability defined over \mathcal{X} , for all $\mathcal{A} \subseteq \mathcal{X}$ we assign a volume $V(\mathcal{A})$. If the element volume of the manifold with coordinates $\mathbf{x} = \{x^1, x^2, \dots, x^k\}$ is $dV_{\mathcal{X}} = v(\mathbf{x}) d\mathbf{x}$, then the volume of a region $\mathcal{A} \subseteq \mathcal{X}$ is

$$V_{\mathcal{A}} = \int_{\mathcal{A}} v(\mathbf{x}) d\mathbf{x} \quad (5)$$

As \mathcal{X} is finite dimensional, the total volume $V_{\mathcal{X}}$ is finite. In effect, if the probability density is normalized with respect to the volume as

$$\mu(\mathbf{x}) = \frac{v(\mathbf{x})}{V_{\mathcal{X}}} \quad (6)$$

then any region $\mathcal{A} \subseteq \mathcal{X}$ is associated with a probability that is proportional to the volume $V_{\mathcal{A}}$. This notion of ‘volumetric

probability’, enables the understanding of the homogeneous probability distribution of a certain event, and although rather trivial in its structure, it plays a significant role in the derivation of the inverse problem theory. According to Tarantola in [22], no coherent inverse theory can be set without the introduction of the homogeneous probability distribution. From a practical point of view, it is only in highly degenerated inverse problems that the particular form of $\mu(\mathbf{x})$ has an impact on the problem. All the probability densities $f(\mathbf{x})$ defined over a set of coordinates \mathbf{x} of manifold \mathcal{X} are considered to be *absolutely continuous* with respect to the homogeneous probability density $\mu(\mathbf{x})$.

In this context, let $\mathcal{S} = \mathcal{X} \times \mathcal{Y}$ be the joint manifold with a homogeneous marginal probability density function

$$\mu(\mathbf{y}, \mathbf{x}) = \mu_{\mathbf{y}}(\mathbf{y})\mu_{\mathbf{x}}(\mathbf{x}) \quad (7)$$

where $\mu_{\mathbf{x}}(\mathbf{x})$ and $\mu_{\mathbf{y}}(\mathbf{y})$ are by definition independent. Allow also the density function that combines the conditional probability density of \mathbf{x} given observations \mathbf{y} according to the EIT model $\theta(\mathbf{y}|\mathbf{x})$ and the marginal $\mu_{\mathbf{x}}(\mathbf{x})$ as

$$\Theta(\mathbf{y}, \mathbf{x}) = \theta(\mathbf{y}|\mathbf{x})\mu_{\mathbf{x}}(\mathbf{x}) \quad (8)$$

Moreover, allow a *prior* probability density $\rho(\mathbf{y}, \mathbf{x})$ defined on the manifold \mathcal{S} reflecting the state of prior information about the data and the solution, so that

$$\rho(\mathbf{y}, \mathbf{x}) = \rho_{\mathbf{y}}(\mathbf{y})\rho_{\mathbf{x}}(\mathbf{x}) \quad (9)$$

under the fundamental assumption that the prior probability densities $\rho_{\mathbf{y}}(\mathbf{y})$ and $\rho_{\mathbf{x}}(\mathbf{x})$ are independent, and thus no correlation between the data and the parameters exists apart from what is included in $\Theta(\mathbf{y}, \mathbf{x})$. When the information content in the data is combined with the available prior information it is easy to derive the *a posteriori* state of information. Applying a conjunction rule on the probabilities we can arrive at the probability density function

$$\sigma(\mathbf{y}, \mathbf{x}) \propto \frac{\rho(\mathbf{y}, \mathbf{x})\Theta(\mathbf{y}, \mathbf{x})}{\mu(\mathbf{y}, \mathbf{x})} \quad (10)$$

from which we can deduce the required a posteriori estimate of the parameters

$$\sigma_{\mathbf{x}}(\mathbf{x}) \propto \rho_{\mathbf{x}}(\mathbf{x}) \int_{\mathcal{Y}} \frac{\rho_{\mathbf{y}}(\mathbf{y})\theta(\mathbf{y}|\mathbf{x})}{\mu_{\mathbf{y}}(\mathbf{y})} \quad (11)$$

A. The Gaussian model

Consider that we are in possession of an array of differential data $\beta = F(\mathbf{x}^\alpha) - \mathbf{y}$ and we seek to recover a perturbation \mathbf{h} in the parameters from a strictly feasible initial estimate of the distribution \mathbf{x}^α . In this, if \mathbf{h} is small enough in norm, so that to be recovered from the linearization of (4) at \mathbf{x}^α , one arrives at the algebraic system

$$F'(\mathbf{x}^\alpha)\mathbf{h} = A\mathbf{h} = \beta \quad (12)$$

where A is a linear, compact and self-adjoint integral operator with a non-closed range, the discrete Fréchet derivative of F evaluated at \mathbf{x}^α .

When the EIT model uncertainties can be described by a Gaussian probability density function with zero mean and standard deviation σ , embedded in a covariance matrix $C_m \succ 0$, where $C \succ 0$ denotes C positive definite, with a well defined inverse and square root, then

$$\theta(\beta|\mathbf{h}) \propto \exp\left(-\frac{1}{2}\|\beta - F(\mathbf{h})\|_{C_m^{-1}}^2\right) \quad (13)$$

If the noise in the data is also Gaussian with zero mean and covariance matrix $C_y \succ 0$ then

$$\rho_y(\beta) \propto \exp\left(-\frac{1}{2}\|\beta\|_{C_y^{-1}}^2\right) \quad (14)$$

and similarly if we further assume that in the linear model space the density function of the prior information on the parameters is multivariate Gaussian with mean \mathbf{h}_p then

$$\rho_x(\mathbf{h}) \propto \exp\left(-\frac{1}{2}\|\mathbf{h} - \mathbf{h}_p\|_{C_x^{-1}}^2\right) \quad (15)$$

where $C_x \succ 0$ is the model prior information covariance matrix and $\mathbf{h}_p \in \text{int}\mathcal{X}$ the prior information guess on the solution. Assuming that \mathbf{h} and ε are independent and importing the relations (13)-(15) into (11) yields,

$$\begin{aligned} \sigma_x(\mathbf{h}) \propto & \exp\left(-\frac{1}{2}(F(\mathbf{h}) - \beta)^T C_d^{-1} (F(\mathbf{h}) - \beta)\right) \cdot \\ & \exp\left(-\frac{1}{2}((\mathbf{h} - \mathbf{h}_p)^T C_x^{-1} (\mathbf{h} - \mathbf{h}_p))\right) \end{aligned} \quad (16)$$

with $C_d = C_m + C_y$. Using (16) and $F(\mathbf{h}) \approx A\mathbf{h}$ the solution we seek to reconstruct corresponds to the point where the a posteriori estimate is maximized, hence the approach leads to a quadratic minimization problem with optimum solution

$$\mathbf{h}^* = \arg \max_{\mathbf{h} \in \mathcal{X}} \sigma_x(\mathbf{h}) \equiv \arg \min_{\mathbf{h} \in \mathcal{X}} f(\mathbf{h}) \quad (17a)$$

where

$$f(\mathbf{h}) = \frac{1}{2} \left\{ \|Q(A\mathbf{h} - \beta)\|_2^2 + \|P(\mathbf{h} - \mathbf{h}_p)\|_2^2 \right\} \quad (17b)$$

where $Q = \sqrt{(C_d)^{-1}} \in \mathbf{R}^{m \times m} \succ 0$ and $P = \sqrt{(C_x)^{-1}} \in \mathbf{R}^{k \times k} \succ 0$. In the above formulation, one should notice that none of the actual covariances is used; indeed it is merely their inverses which are introduced in the construction of the problem. In fact, C_x , C_y and C_d may not even exist or their densities may be improper, however the existence of their inverses simply imposes that fact that there is no linear combination of the random variables, parameters or data, that has a vanishing variance [12].

Ill-posed problems are notorious for their exhibited instability when these are attempted in the framework of unconstrained optimization algorithms [7], [9]. Consider for instance, the case where the data are infused with some Gaussian noise, the EIT model is thought to be exact and there is no available prior information about the data or the solution. In such occasion, $\rho_y(\mathbf{y}) = \mu_y(\mathbf{y})$ and $\rho_x(\mathbf{x}) = \mu_x(\mathbf{x})$ and the space of the data becomes a finite subset of the space of square integrable functions, $\mathcal{Y} \subset L^2(\Omega)$ effectively

reducing the linearized inverse problem into a minimum norm problem whose solution

$$\mathbf{h}^\dagger = \arg \min_{\mathbf{h} \in \mathbf{R}^k} \frac{1}{2} \|A\mathbf{h} - \beta\|_2^2 \quad (18)$$

also referred to as the Moore-Penrose solution, is unbounded in norm in \mathcal{X} [7], [2], [22]. In effect, ill-posed problems can only be cast in the framework of constrained optimization [3]. Due to the ill-posedness of the problem, the discrete Fréchet derivative of the forward operator $F: \mathcal{X} \rightarrow \mathcal{Y}$ evaluated in the interior of \mathcal{X} , is an ill-conditioned matrix with exponentially decaying eigenvalues. In fact, it is safe to assume that in general A has a cluster of nearly zero singular values, and thus with respect to the level of precision in the data, it is effectively rank deficient. From the singular value decomposition (SVD) of $A \in \mathbf{R}^{m \times k}$, assuming $m \leq k$

$$A = USV^T \quad (19)$$

where $U \in \mathbf{R}^{m \times m}$ and $V \in \mathbf{R}^{k \times k}$ are the orthogonal matrices holding the singular vectors in \mathcal{X} and \mathcal{Y} so that $U^T U = I$ and $V^T V = I$ and $S \in \mathbf{R}^{m \times k}$ is the diagonal with the singular values of A in descending order, we can obtain the nontrivial null space of A

$$\mathcal{N}(A) = \{s_i | s_i \leq w\} \neq \emptyset \quad (20)$$

and write the solution to (18) as a sum of the singular functions weighted by the measurements

$$\mathbf{h}^\dagger = \sum_{i=1}^m \frac{\langle u_i, \beta \rangle_{\mathcal{Y}}}{s_i} v_i \quad (21)$$

where $\langle \cdot, \cdot \rangle_{\mathcal{Y}}$ the inner product in \mathcal{Y} and $s_i \sim O(e^{-2i})$. For the solution to remain bounded the Picard criterion [18] imposes that the coefficients $\langle u_i, \beta \rangle_{\mathcal{Y}}$ should decay faster than s_i . If the data vector is split into the exact and noisy components like $\beta = \beta^{exact} + \varepsilon$, we can write the minimum norm solution in terms of the ‘correct’ and the ‘erroneous’ components

$$\mathbf{h}^\dagger = \sum_{i=1}^m \frac{\langle u_i, \beta^{exact} \rangle_{\mathcal{Y}}}{s_i} v_i + \sum_{i=1}^m \frac{\langle u_i, \varepsilon \rangle_{\mathcal{Y}}}{s_i} v_i \quad (22)$$

As $i \rightarrow m$ both components seemingly increase as $s_i \rightarrow 0$. In the high frequency region, i.e. $i \sim m$, the coefficients $\langle u_i, \beta^{exact} \rangle_{\mathcal{Y}}$ reduce to zero due to the smoothing kernel of the Laplacian operator in the EIT model which essentially makes $\beta^{exact} = F(\mathbf{h}^*)$ a low frequency smooth function. In contrast, the values of $\langle u_i, \varepsilon \rangle_{\mathcal{Y}}$ rise asymptotically and along with the small singular values cause \mathbf{h}^\dagger to grow unbounded. This is graphically illustrated in the Picard plot shown in figure 2. This result which relates to the compactness of the elliptic operator A is fundamental in the theory of linear ill-posed inverse problems and we state it next for completeness.

Definition 3.1: A linear operator A from a Hilbert space \mathcal{X} to a Hilbert space \mathcal{Y} is said to be *compact* if it maps bounded sets in \mathcal{X} to relatively compact sets in \mathcal{Y} .

Theorem 3.2: Suppose $A : \mathcal{X} \rightarrow \mathcal{Y}$ where \mathcal{X} and \mathcal{Y} are Hilbert spaces, is linear, bounded and therefore compact operator. Suppose in addition that \mathcal{X} is not finite dimensional. Then $A^{-1} : \mathcal{Y} \rightarrow \mathcal{X}$, if it exists, cannot be bounded.

Proof: The compactness of A is a direct consequence of the Arzela-Ascoli theorem which can be found in [27]. Here we sketch a less rigorous proof based on contradiction. Suppose the inverse A^{-1} exists and is bounded. Then $A^{-1}A$ is also compact since the product of a bounded and a compact operator is compact. For this to hold \mathcal{X} must be finite dimensional and I should not be invertible. Consequently, A^{-1} must be unbounded and discontinuous. In corollary, the linearized problem is ill-posed, violating Hadamard's third criterion for well-posedness [7]. In the discrete case, A yields an ill-conditioned matrix with exponentially decreasing singular values. This completes the proof. ■

IV. FORMULATING THE PRIMAL PROBLEM

Taking a first-order approximation approach by neglecting $O(\mathbf{h}^2)$ terms and above in the Taylor expansion of F we proceed to consider the linearized regularized inverse problem

$$\min_{\mathbf{h} \in \mathbf{R}^k \cap \{\mathbf{h} \mid \|P(\mathbf{h} - \mathbf{h}_p)\|_2^2 \leq t\}} \frac{1}{2} \|Q(A\mathbf{h} - \beta)\|_2^2 \quad (23)$$

where the inequality constraint imposes that the linear step solution has a P -norm with upper bound t . The common approach to this problem is to cast it as a bi-criterion optimization problem following the ideas suggested by Boyd et al [3] and Golub et al. [8], effectively combing the Q -weighted least-squares and the inequality ℓ_2 norm terms in a Lagrangian function. In his monumental work on the problem, Tikhonov [23] showed that the problem (23) admits a unique and stable regularized solution which has the analytic form

$$\mathbf{h}_{tik} = (A^T C_d^{-1} A + C_x^{-1})^{-1} A^T C_d^{-1} \beta \quad (24)$$

Assuming high quality instrumentation for the collection of the data, so that the noise in the measurements is uncorrelated and normally distributed around zero, and a negligible amount of model uncertainty, the Tikhonov solution reduces to

$$\mathbf{h}_{tik} = (A^T A + \tau P^T P)^{-1} (A^T \beta + \tau P^T P \mathbf{h}_p) \quad (25)$$

where $\tau \in \mathbf{R}$ the strictly positive regularization parameter that weights the two norms in (23). Although, the method is quite popular for this type of problems and it is often preferred for its direct implementation, see also the applications in [9] and [25], it presents a fundamental difficulty; that of computing the optimum value of the parameter τ . This has been the subject of intense research activity in the field of inverse problems and various numerical techniques have been suggested, among which the L-curve criterion by Hansen [9] and the generalized cross validation method by Nguyen et al. [15] essentially relating the parameter to

the error level in the data. Effectively, if $0 < \gamma_1 \leq \gamma_2 \leq \dots \leq \gamma_{\min(m,k)} < \infty$ are the generalized singular values of the pair (A, P) , so that $A = USX^T$, $P = VCX^T$ and $\gamma_i = c_i + s_i$ satisfying $C^T C + S^T S = I$, the optimum parameter τ is known to be situated in the interior of the interval $[w, \gamma_1]$ [18].

From a numerical prospective, Tikhonov regularization performs a smooth ℓ_2 low-pass filtration in the singular values of A thereby suppressing the high frequency components of (A, P) , that is mainly γ_i and u_i for large i . In doing so, it performs a systematic truncation on the eigenfunctions of the solution, removing not only the noise amplification but the high frequency components of the solution itself, like sharp edges and detailed features, effectively compromising the spatial resolution in the reconstructed images in order to preserve stability. The amount of filtration in the singular values is decided upon the choice of the regularization parameter τ , for which we can define the so-called Tikhonov filters

$$\hat{f}_i = \frac{\gamma_i^2}{\gamma_i^2 + \tau} \quad i = 1 : \min(m, k)$$

in which case if the effective rank of A is $r < \min(m, k)$, the generalized Tikhonov solution takes the form

$$\mathbf{h}_{tik} = \sum_{i=1}^r \hat{f}_i \frac{\langle u_i, \beta \rangle_{\mathcal{Y}}}{s_i} X_i + \sum_{i=r+1}^k \langle u_i, \beta \rangle_{\mathcal{Y}} X_i \quad (26)$$

Notice that the low-pass filters operate by comparing the value of the generalized singular value to the choice of the regularization parameter, like

$$\gamma_i \gg \tau \Rightarrow \hat{f}_i \sim 1 \quad \text{and} \quad \gamma_i \ll \tau \Rightarrow \hat{f}_i \sim 0 \quad (27)$$

Finding the optimal value of τ so that to optimize the filtration is quite a hard problem in its own merits, as Rojas et al. point out in [20] and [19]. The reports proceed to explain that apart from controlling the inconsistencies in the data and the model, the regularization parameter should also measure the conformance of the probabilistically chosen prior information, and therefore provide an estimate of how much the regularized problem deviates from its original ill-posed counterpart. Intuitively, from (25) and (22) it follows that τ^* should decay to zero as $w \rightarrow 0$, causing \mathbf{h}^\dagger and \mathbf{h}_{tik} to coincide. Despite being a bi-criterion optimization problem in its origins, in many respects the Tikhonov problem can be thought of as a least squares problem with an always-binding inequality constraint, in which case its solution can be easily shown to satisfy the appropriate Lagrange function. This approach, also used in [8], is adopted for the derivation of the primal and dual inverse impedance problems next.

V. THE PRIMAL AND DUAL INVERSE PROBLEMS

Let $f : \mathbf{R}^k \rightarrow \mathbf{R}$, $g : \mathbf{R}^k \rightarrow \mathbf{R}$, where g is convex and f is non-convex. If $f = \frac{1}{2} \|Q(A\mathbf{h} - \beta)\|_2^2$ and $g = \frac{1}{2} \|P(\mathbf{h} - \mathbf{h}_p)\|_2^2$, then the primal Tikhonov problem is

$$\min_{\mathbf{h} \in \mathcal{X}, g(\mathbf{h}) \leq t} f(\mathbf{h}) \quad (28)$$

The Lagrange function $\mathcal{L} : \mathbf{R}^k \times \mathbf{R} \rightarrow \mathbf{R}$ of the problem is

$$\begin{aligned}\mathcal{L}(\mathbf{h}, \lambda) &= f(\mathbf{h}) + \lambda(g(\mathbf{h}) - t) \\ &= \frac{1}{2}\mathbf{h}^T A_q \mathbf{h} - c^T \mathbf{h} + \frac{1}{2}\beta^T Q^T Q \beta \\ &\quad + \frac{\lambda}{2} \left[(\mathbf{h}^T P^T P \mathbf{h} - 2\mathbf{h}^T P^T P \mathbf{h}_p + \|\mathbf{P}\mathbf{h}_p\|_2^2) - t \right]\end{aligned}\quad (29)$$

with $A_q = A^T Q^T Q A$, $c = A^T Q^T Q \beta$, and infimum $\mathbf{h}^* = (A_q + \lambda P^T P)^{-1} c$ at $\nabla_{\mathbf{h}} \mathcal{L} = 0$, and if $p(t) = \mathbf{h}^*$ is the optimum primal solution given by

$$p(t) = \inf_{\mathbf{h} \in \mathcal{X}, g(\mathbf{h}) \leq t} f(\mathbf{h})$$

and R the domain of the primal function so that

$$R = \{t \mid \mathbf{h} \in \mathcal{X}, g(\mathbf{h}) \leq t, p(t) < \infty\} \neq \emptyset$$

then for all dual multipliers $\lambda \geq 0$, the dual function takes the form

$$\begin{aligned}q(\lambda) &= \inf_{\mathbf{h} \in \mathcal{X}} \left\{ f(\mathbf{h}) + \lambda g(\mathbf{h}) \right\} \\ &= \inf_{\{(t, \mathbf{h}) \mid t \in R, \mathbf{h} \in \mathcal{X}, g(\mathbf{h}) \leq t\}} \left\{ f(\mathbf{h}) + \lambda g(\mathbf{h}) \right\} \\ &= \inf_{\{(t, \mathbf{h}) \mid t \in R, \mathbf{h} \in \mathcal{X}, g(\mathbf{h}) \leq t\}} \left\{ f(\mathbf{h}) + \lambda t \right\}\end{aligned}$$

yielding the dual problem [1]

$$\begin{aligned}\inf_{\lambda \geq 0} \inf_{t \in R} \{p(t) + \lambda t\} &\equiv \\ \max_{\lambda \geq 0, A_q + \lambda P^T P \succeq 0} -\frac{1}{2} \tilde{c}^T (A_q + \lambda P^T P)^{-1} \tilde{c} - \frac{\lambda}{2} t\end{aligned}\quad (30)$$

where $\tilde{c} = c + \lambda \mathbf{h}_p P^T P$. The optimum inverse solution is the point on the surface of a spherical trust-region $\|g(\mathbf{h})\|_2^2 = t$ with radius t , where the composite function $\{\lambda \|g(\mathbf{h})\|_2^2 + \|f(\mathbf{h})\|_2^2\}$ attains its infimum. By a trivial manipulation we can transform the primal (28) into an unconstrained minimization problem with an objective term $\Phi(\mathbf{h}, \lambda)$ convex in \mathbf{h} and concave-linear in λ like

$$\inf_{\mathbf{h} \in \mathcal{X}} \Phi(\mathbf{h}, \lambda) \quad (31)$$

where

$$\Phi(\mathbf{h}, \lambda) = \frac{1}{2} \mathbf{h}^T (A_q + \lambda P^T P) \mathbf{h} - (c^T + \lambda \mathbf{h}_p P^T P) \mathbf{h} - \frac{\lambda}{2} t \quad (32)$$

VI. OPTIMALITY CONDITIONS

A point (\mathbf{h}, λ) is considered to be the optimum solution of the problem (23) iff it satisfies the first-order KKT conditions of optimality

$$(A_q + \lambda P^T P) \mathbf{h} = c + \lambda \mathbf{h}_p P^T P \quad (33a)$$

$$S(\lambda, \mathbf{h}) = \frac{\lambda}{2} \left(\|P(\mathbf{h} - \mathbf{h}_p)\|_2^2 - t \right) = 0 \quad (33b)$$

$$\lambda \geq 0 \quad (33c)$$

and the Hessian of the convex $\Phi(\mathbf{h}, \lambda)$

$$(A_q + \lambda P^T P) \succ 0 \quad (33d)$$

is positive definite for all $\mathbf{h} \in \mathcal{X}$.

VII. THE INTERIOR POINT TRUST-REGION ALGORITHM

For the inverse problem, we implement a primal-dual interior point trust-region algorithm, considering a total of $k+1$ degrees of freedom for a model with k parameters of interest [19]. Perturbing the optimality conditions (33) we derive the primal-dual Newton system of equations

$$\begin{aligned}H(\Phi) \begin{bmatrix} \delta \mathbf{h} \\ \delta \lambda \end{bmatrix} &= -D(\Phi) \\ (\mathbf{h}, \lambda) &\leftarrow (\mathbf{h}, \lambda) + \nu (\delta \mathbf{h}, \delta \lambda)\end{aligned}\quad (34a)$$

where $\nu > 0$ is the size of the step length in the the dual direction and the primal-dual Hessian $H(\Phi) \in \mathbf{R}^{k+1 \times k+1}$ has the form

$$\begin{aligned}H(\Phi) &= \begin{bmatrix} \nabla_{\mathbf{h}}(\nabla_{\mathbf{h}} \mathcal{L}) & \nabla_{\lambda}(\nabla_{\mathbf{h}} \mathcal{L}) \\ \nabla_{\mathbf{h}} S & \nabla_{\lambda} S \end{bmatrix} \\ &= \begin{bmatrix} A_q + \lambda P^T P & P^T P(\mathbf{h} - \mathbf{h}_p) \\ \lambda (P^T P(\mathbf{h} - \mathbf{h}_p)) & \frac{1}{2} \|P(\mathbf{h} - \mathbf{h}_p)\|_2^2 - t \end{bmatrix}\end{aligned}\quad (34b)$$

Similarly, the perturbed primal-dual gradient $D(\Phi) \in \mathbf{R}^{k+1}$ is given by

$$D(\Phi) = \begin{bmatrix} \nabla_{\mathbf{h}} \mathcal{L} \\ S - \mu \end{bmatrix} = \begin{bmatrix} (A_q + \lambda P^T P) \mathbf{h} - c - P^T P \mathbf{h}_p \\ \frac{\lambda}{2} \left(\|P(\mathbf{h} - \mathbf{h}_p)\|_2^2 - t \right) - \mu \end{bmatrix} \quad (34c)$$

where $\mu > 0$ is the interior point method parameter which decays asymptotically $\mu \rightarrow 0_+$ as the optimum point is approached $(\mathbf{h}, \lambda) \rightarrow (\mathbf{h}^*, \lambda^*)$.

VIII. CONCLUSIONS AND FUTURE WORK

In this work we have derived the primal and dual problems in Tikhonov regularization and suggested a trust-region interior point algorithm for their optimal solution. We have demonstrated how the inverse conductivity can be reconstructed while optimizing the Tikhonov regularization parameter at the same time.

Implementing a Gaussian model for the uncertainty in the model, the noise in the boundary measurements and the prior information on the solution, yields analytic expressions for the inverse solution as the conjunction of the probabilities is radically simplified by the presence of the exponentials in the associated probability density functions. Nonetheless, we anticipate that interesting analysis and results will arise by considering alternative probability densities which reflect more sophisticated priors about the conductivity and noise signals. An alternative noise covariance for example, may be more appropriate to resemble the noise signal in industrial experiments where insufficient insulation in the measuring leads encourages noise correlation.

REFERENCES

- [1] D.P. Bertsekas, *Nonlinear programming*, second ed., Athena Scientific, Massachusetts, 2004.
- [2] L. Borcea, *Review: Electrical impedance tomography*, *Inverse Problems* **18** (2002), no. 6, R99–R136.
- [3] S. Boyd and L. Vandenberghe, *Convex optimization*, Cambridge University Press, New York, 2004.
- [4] B.H. Brown, *Medical impedance tomography and process impedance tomography: a brief review*, *Measurement Science and Technology* **12** (2001), 991–996.

- [5] A. P. Calderón, *On an inverse boundary value problem. seminar on numerical analysis and its applications to continuum physics*, Proceedings of Society Brasileira de Matemática (1980), 65–73.
- [6] M. Cheney, D. Isaacson, and J.C. Newell, *Electrical impedance tomography*, SIAM Review **41** (1999), no. 1, 85–101.
- [7] H.W. Engl, M. Hanke, and A. Neubauer, *Regularization of inverse problems*, Mathematics in Industrial Applications, Kluwer Academic, 1997.
- [8] G. Golub, P.C. Hansen, and D.P. O’Leary, *Tikhonov regularization and total least squares*, SIAM Journal of matrix analysis and applications **21** (1999), no. 1, 185–194.
- [9] P. C. Hansen, *Rank-deficient and discrete ill-posed problems: Numerical aspects of linear inversion*, SIAM, 1999.
- [10] D. S. Holder, *Electrical impedance tomography: Methods, history and applications*, Institute of Physics, Bristol, 2004.
- [11] J. Jin, *The finite element method in electromagnetics*, second ed., Wiley Interscience, New York, 2002.
- [12] J.P. Kaipio, A. Seppänen, E. Somersalo, and H. Haario, *Posterior covariance related optimal current patterns in electrical impedance tomography*, Inverse Problems **20** (2004), 919–936.
- [13] W.R.B. Lionheart, *Boundary shape and electrical impedance tomography*, Inverse Problems **14** (1998), no. 1, 139–147.
- [14] ———, *Review: Developments in EIT reconstruction algorithms: pitfalls, challenges and recent developments*, Physiological Measurement **25** (2004), 125–142.
- [15] N. Nguyen, P. Milanfar, and G. Golub, *Efficient generalized cross-validation with applications to parametric image restoration and resolution enhancement*, IEEE Transactions on image processing **10** (2001), no. 9, 1299–1308.
- [16] K.S. Paulson, W.R. Breckon, and M.K. Pidcock, *Electrode modelling in electrical impedance tomography*, SIAM Journal of Applied Mathematics **52** (1992), 1012–1022.
- [17] N. Polydorides and W.R.B. Lionheart, *A matlab toolkit for three dimensional electrical impedance tomography: A contribution to the eidors project*, Measurement Science and Technology **13** (2002), no. 12, 1871–1883.
- [18] N. Polydorides and H. McCann, *Electrode configurations for improved spatial resolution in electrical impedance tomography*, Measurement Science and Technology **13** (2002), no. 12, 1862–1870.
- [19] M. Rojas and D.C. Sorensen., *A trust-region approach to the regularization of large-scale discrete forms of ill-posed problems*, SIAM Journal on Scientific Computing **26** (2002), no. 3, 1843–1861.
- [20] M. Rojas and T. Steihaug, *An interior-point trust-region-based method for large-scale non-negative regularization*, Inverse problems **18** (2002), no. 5, 1291–1307.
- [21] E. Somersalo, M. Cheney, and D. Isaacson, *Existence and uniqueness for electrode models for electric current computed tomography*, SIAM Journal of Applied Mathematics **52** (1992), no. 4, 1023–1040.
- [22] A. Tarantola, *Inverse problems theory and methods for model parameter estimation*, SIAM, Philadelphia, 2004.
- [23] A. Tikhonov and V. Arsenin, *Solutions of ill-posed problems*, John Wiley, New York, 1977.
- [24] P.J. Vauhkonen, M. Vauhkonen, T. Savolainen, and J.P. Kaipio, *Three-dimensional electrical impedance tomography based on the complete electrode model*, IEEE Transactions on Biomedical Engineering **46** (1999), no. 9, 1150–1159.
- [25] C. Vogel, *Computational methods for inverse problems*, SIAM, Philadelphia, 2002.
- [26] R.A. Williams and M.S Beck, *Process tomography: Principles, techniques and applications*, Butterworth-Heinemann, Oxford, 1995.
- [27] K. Yosida, *Functional analysis*, sixth ed., Comprehensive studies in Mathematics, Springer-Verlag, Berlin, 1980.

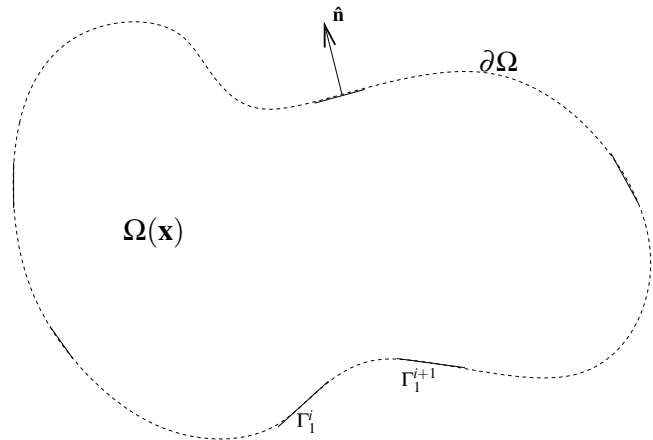


Fig. 1. The schematic diagram of an EIT system, showing a domain Ω of conductivity distribution \mathbf{x} , having a boundary $\partial\Omega$ and an outward unit normal vector $\hat{\mathbf{n}}$. the diagram illustrates also the array of boundary electrodes $\Gamma_1 = \bigcup_{i=1}^L \Gamma_1^i$ and the inter-electrode gap $\Gamma_2 = \partial\Omega \setminus \Gamma_1$.

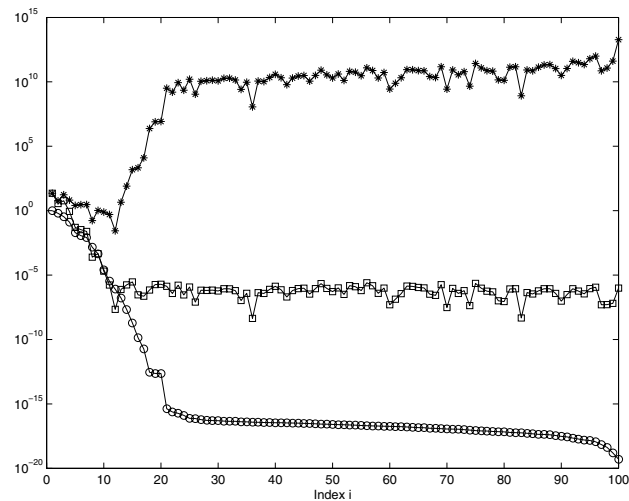


Fig. 2. The Picard plot for a typical example of an EIT problem with 100 measurements infused with a noise signal of $\sigma = 10^{-6}$. The (o) line shows the normalized exponentially decreasing singular values s_i , $i = 1 : 100$ of A , the (□) plot connects the corresponding absolute values of the coefficients $\langle u_i, \beta \rangle_{L^2(\Omega)}$ and the (*) line the associated i 'th components of \mathbf{h}^\dagger .